

## CHAPTER 233

# Water Wave Propagation in Jettied Channels

Robert A. Dalrymple<sup>1</sup>, F., ASCE

### Abstract

Navigational channels are frequently maintained by the use of jetties. These stabilized channels often form long straight waterways which permit the passage of tidal flows and waves into harbors, lagoons, or rivers. This paper concerns the decay of the waves down the channel due to energy losses within jetties. The analysis involves the use of an impedance boundary conditions at the channel side walls to model the wave dissipation there. The wave motion is described by an eigenfunction expansion for the velocity potential within the channel, with and without tidal currents.

For the case that the water wave length is long with respect to the channel width and no currents are present, the wave height decay down the channel can be described by an exponential decay,  $H = H_0 e^{-\Gamma x}$ , where  $\Gamma = \gamma x / (2kb)$ ,  $\gamma$  is a (real) damping factor,  $k$  is the wave number, and  $2b$  is the width of the channel. For the case of a mean current in the channel, the same expression results, but for a different form of the wave number, (Eq. 24).

### Introduction

Stabilized entrance channels often form long straight waterways which permit the passage of tidal flows and water waves into harbors or lagoons. This paper concerns the interaction of water waves with rubble mound jetties, including the significant energy loss into the jetties, due to turbulent energy dissipation.

The energy decay down a channel may be calculated if the rates of energy loss are known at the bottom and the sides of the channel. The conservation of energy flux down the channel is

$$\frac{d\mathcal{F}}{dx} = -\mathcal{D} \quad (1)$$

---

<sup>1</sup>Professor and Director, Center for Applied Research, Department of Civil Engineering, Univ. Delaware, Newark, DE 19716

where the wave energy flux is  $\mathcal{F} = EC_g(2b) = \frac{1}{4}\rho g H^2 C_g b$ , where  $\rho$  is the fluid density,  $g$  is the acceleration of gravity,  $H$ , the wave height in the channel,  $C_g$  is the group velocity of the waves, and  $b$  is the half-width of the channel.  $\mathcal{D}$  is the energy dissipation per unit length of channel. This expression can be rewritten as

$$\frac{dH}{dx} = -\frac{2\mathcal{D}}{\rho g H C_g b} \quad (2)$$

Hunt (1952) examined the decay of wave height due to laminar boundary layers at the sides and the bottom of a rectangular impermeable channel. In this case,  $\mathcal{D}$  is proportional to  $H^2$ , and therefore Eq. 2 can be written as

$$\frac{dH}{dx} = -\Gamma H \quad (3)$$

which leads to the following expression for wave height down the channel,

$$H(x) = H_o e^{-\Gamma x} \quad (4)$$

where  $\Gamma$  depends on the viscosity of the fluid as well as the other factors.

Battjes (1965) studied the damping of waves in a rectangular wave channel with roughness strips attached to the sidewalls along the length of the channel. The strips were mounted vertically over the depth on the sides of the channel with a fixed spacing. Vortices shed by the wave-induced flow past the strips resulted in a decrease in wave height down the channel. Battjes examined a 'turbulent damping' such that the dissipation as the side walls was assumed to be proportional to  $H^3$ ,

$$\frac{dH}{dx} = -\beta H^2 \quad (5)$$

leading to

$$H = \frac{H_o}{(1 + \beta H_o x)} \quad (6)$$

The experiments were conducted in an approximately 27.5 m long, 3.0 m wide test section of the channel. To get an adequate decay distance, the wave height at the end of the test section after one run, was used as the input to another test. By coupling experiments in this fashion, data on wave height versus distance was generated for an equivalent tank, 6 to 7 times longer. However, since the phenomenon he discusses is nonlinear and cross-tank oscillations occur, it is not likely that this is a valid experimental approach.

Isaacson (1978) applied the same formula as Battjes for the wave height down a prismatic trapezoidal entrance channel laboratory model lined with stone, varying the side slopes. He found that there was a strong dependency of  $\beta$  on wave period, with  $\beta$  increasing with period.

Melo and Guza (1991a,b) in an interesting computational and field study showed that the wave height down the centerline of an entrance channel decreased rapidly, mostly due to the diffraction of the waves into the absorbing jetty structures. They also point out that the diffraction through a breakwater gap of the same width as the entrance channel gives similar damping behavior down the centerline. If the channel is narrow with respect to the wave length of the incident waves, then the diffractive damping is more severe, as discussed by Losada *et al.* (1990). The computational analysis of Melo and Guza consisted of two coupled parabolic models of wave propagation, one in the channel and another within the porous structure, with matching conditions on the jetty face for velocity and pressure.

The intent of this paper is to develop a new methodology for computing the wave field within navigational channels without having to use coupled parabolic wave models (as in Melo and Guza) through the use of the impedance boundary condition.

### Theory

The wave motion will be described within the jetty section, assuming that the wave height is specified across the mouth of the channel. Figure 1 shows the channel and the coordinate system to be used in the analysis. The channel is assumed here to be constant in depth, which simplifies the analysis.

Between the jetties, which are located at  $y = \pm b$ , the wave motion is assumed to be described by linear wave theory which results from the assumption of small amplitude irrotational wave motion within an incompressible fluid. The associated governing equation is the Laplace equation for a velocity potential  $\phi(x, y, z, t)$ ,

$$\nabla^2 \phi = 0 \quad (7)$$

from which the velocities in the fluid can be determined,  $\mathbf{u} = (u, v, w) = -\nabla \phi$ . At the bottom boundary, no flow is permitted,

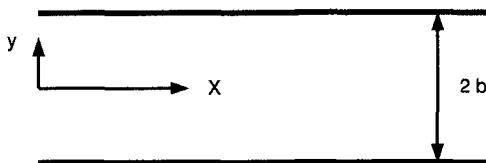


Figure 1: Schematic of Channel

$$-\frac{\partial\phi}{\partial z} = 0 \quad \text{on } z=0. \tag{8}$$

At the jetties, an impedance boundary condition is assumed,

$$\frac{\partial\phi}{\partial y} = i\gamma\phi = ik\beta\phi \quad \text{on } y = |b| \tag{9}$$

where  $\gamma$  is  $k$  (the wave number) times the *specific admittance*,  $\beta$ , of the jetties. This assumption follows from acoustics, where it is used to determine the damping of acoustic waves due to absorbent duct boundaries (e.g. Morse and Ingard, 1968, §6.3). If  $\gamma$  is real, then wave energy is absorbed by the jetties; for  $\gamma$  purely imaginary, this boundary condition leads to 100% reflection with a phase shift. The value of  $\gamma$  (or equivalently the dimensionless  $\beta$ ) will strongly dictate the nature of the solution and its value will be specified later.

The impedance boundary condition on the jetties can be compared to a transmitting condition for plane waves, usually imposed on an open coast model (e.g., Kirby, 1985), which is taken as

$$\frac{\partial\phi}{\partial y} = ik \sin \theta\phi \tag{10}$$

where  $\theta$  is the angle of the wave direction to the  $x$  axis. Comparing to (9), the specific admittance for a transmitting boundary is  $\beta = \sin \theta$ , which varies from 0 to 1. The value of  $\gamma$  then must be less than the wave number,  $k$ , as it implies that waves are normally incident on the jetties and fully transmitting through them.

For the general case, an equivalent admittance will be defined as  $\sin \theta$  when  $\beta$  is real.

### Eigenfunction Expansion

The velocity potential in the channel will be similar to that used by Dalrymple (1989), studying ‘designer waves’ for directional wavemakers. In general, the total potential will consist of even and odd eigenfunction components, across the channel, but here we will restrict ourselves to normally incident wave trains, so that only the even modes will be utilized. The potential (in the absence of a mean flow in the channel) is therefore assumed to be

$$\phi(x, y, z, t) = \sum_{n=1}^{\infty} C_n \cos \lambda_n y \frac{\cosh k(h+z)}{\cosh kh} e^{i(\sqrt{k^2-\lambda_n^2}x-\sigma t)} \tag{11}$$

where the set  $\{\cos \lambda_n y\}$  is an anharmonic (orthogonal) Fourier series in  $y$ , and the usual linear wave theory dispersion relationship holds:

$$\sigma^2 = gk \tanh kh, \tag{12}$$

which relates the wave number  $k$  and the water depth and wave angular frequency,  $\sigma = 2\pi/T$ , where  $T$  is the wave period.

The lateral boundary conditions (9) place the following constraints on the  $\lambda_n$  in the Fourier series,

$$-\lambda_n \tan \lambda_n b = i\gamma \quad n = 1, 2, \dots \quad (13)$$

which is a transcendental equation to determine the wave numbers  $\lambda_n$  in the lateral direction. (Note that if  $\gamma$  is zero, then the  $\lambda_n = n\pi/b$ .) This boundary condition leads to the orthogonality of the Fourier series:

$$\int_{-b}^b \cos \lambda_n y \cos \lambda_m y \, dy = \begin{cases} 0, & \text{for } n \neq m, \\ \frac{2\lambda_n b + \sin 2\lambda_n b}{2\lambda_n}, & \text{for } n = m. \end{cases} \quad (14)$$

The velocity potential (11) is composed of an infinite number of wave trains, consisting of wave trains which are 'standing' in the cross-channel direction and either propagating or decaying in the down-channel direction. In fact, only a few terms in  $\phi$  represent propagating wave trains as, for large values of  $n$ , the real part of  $\sqrt{k^2 - \lambda_n^2}$  becomes negative and results in a strongly damped motion in the  $x$  direction. In fact, for incident wave trains with wave lengths larger than  $2b$  (the channel width), or  $kb < \pi$ , then only one wave mode ( $n = 1$ ) propagates down the channel (this is strictly true for  $\gamma = 0$ ; but it serves as a guide).

The values of  $C_n$  are determined by the initial value of  $\phi(0, y, t)$ . By orthogonality of the set  $\{\cos \lambda_n y\}$  over  $-b < y < b$ , we find

$$C_n = \frac{2\lambda_n \int_{-b}^b \phi(0, y, t) \cos \lambda_n y \, dy}{2\lambda_n b + \sin 2\lambda_n b} \quad (15)$$

For a given incident wave train of frequency  $\sigma$ ,  $\phi(0, y, t)$  is taken as unity across the mouth of the channel, and the  $C_n$  can be reduced to

$$C_n = \frac{4 \sin \lambda_n b}{2\lambda_n b + \sin 2\lambda_n b} \quad (16)$$

This initial condition imposes phases on the various wave modes (more on this later).

Examining narrow channels, ( $\gamma b \ll 1$ ) and  $kb < \pi$ , the lateral boundary condition (13) can be approximated for  $\lambda_1$ ,

$$\lambda_1^2 = -i\gamma/b \quad (17)$$

The leading term of  $\phi$  is

$$C_1 \cos \lambda_1 y \frac{\cosh k(h+z)}{\cosh kh} e^{i(\sqrt{k^2 - \lambda_1^2} x - \sigma t)} \quad (18)$$

Introducing the approximation for  $\lambda_1$  yields for the approximate wave decay

$$e^{-\left(\frac{\gamma_r}{2bk}\right)x} = e^{-\left(\frac{\beta_r}{2b}\right)x} \tag{19}$$

as  $C_1$  asymptotically goes to unity. Here, the subscript  $r$  denotes the real part. Comparing with the linear damping formula, (4),  $\Gamma = \gamma_r x / 2bk$ . Therefore, the wave height in a channel decreases exponentially down the channel according to this theory. Further, the damping is inversely proportional to  $b$ , the channel half-width.

Alternatively, since  $\lambda_1^2 \ll k^2$ , the exponential term in  $x$  can be approximated as

$$e^{i\sqrt{k^2 - \lambda_1^2}x} \rightarrow e^{ikx} e^{(\lambda_1)_r(\lambda_1)_i x/k}$$

Thus, given the real and (negative) imaginary parts of  $\lambda_1$ , found from (13), the decay of the first wave mode with  $x$  can be found as

$$e^{(\lambda_1)_r(\lambda_1)_i x/k} \tag{20}$$

Since this expression is based on the lateral boundary condition, rather than an approximation, it is more accurate than that provided in (19).

Effects of Tidal Currents

The previous results were obtained for the case of no currents in the channel. However, it is likely for a majority of the tidal cycle there will be a slowly varying flow in the channel or a current due to a river discharge. Therefore the effects of the currents on the wave field and the damping in the channel must be determined.

To include the current (with uniform speed  $U$ , with  $U \gg |\nabla\phi|$ ), the velocity potential is changed to

$$\phi(x, y, z, t) = \phi_c + \phi_w = -Ux + \sum_{n=1}^{\infty} C_n \cos \lambda_n y \frac{\cosh k_n(h+z)}{\cosh k_n h} e^{i(\sqrt{k_n^2 - \lambda_n^2}x - \sigma t)} \tag{21}$$

where the  $\lambda_n$  satisfy the same impedance relationship (9) as before; however,  $\gamma$  may be different than for the no-current case. Also, the dispersion relationship for the wave number results in a different wave number for each wave mode, due to the wave-current interaction, which depends on the wave direction,

$$\left(\sigma - U\sqrt{k_n^2 - \lambda_n^2}\right)^2 = gk_n \tanh k_n h, \quad n = 1, 2, 3, \dots \tag{22}$$

due to the effects of the current on the linear combined free surface boundary condition (e.g., Dean and Dalrymple, 1991, § 3.4.5)

$$\frac{\partial^2 \phi_w}{\partial t^2} + 2U \frac{\partial^2 \phi_w}{\partial x \partial t} + U^2 \frac{\partial^2 \phi_w}{\partial x^2} + g \frac{\partial \phi_w}{\partial z} = 0 \quad \text{on } z = 0 \tag{23}$$

where  $\phi_w$  is the portion of the velocity potential describing the wave motion. The resulting wave numbers ( $k_n$ ,  $n = 1, 2, 3, \dots, \infty$  from 22) are all complex.

For narrow channels, a similar approximation to (19) can be made for the case of waves on currents. This leads to the following relationship for wave height decay down a channel (for normal wave incidence)

$$e^{-\left(\frac{\gamma_r}{2bk_1}\right)x} \quad (24)$$

where  $k_1$  is given by (22).

### Results and Comparisons to Field and Laboratory Data

Figure 2a shows the instantaneous wave field ( $\eta(x, y) = -(i\sigma/g)\phi(x, y, 0)$ ) and the absolute value of  $\eta$  in a channel with the following characteristics:  $b = 120$  m,  $T = 12$  s,  $h = 8$  m, and specific admittance is 0.156, which is  $\gamma = 0.012$  m<sup>-1</sup>. For this case, the curvature of the wave crests is clear with the waves turning into the jetties by diffraction. For this example, the equivalent transmission angle is 8°.

The absolute value of the water surface is contoured in Fig. 2b, with the contours spaced by 0.1. The initial condition of normally incident waves with unit amplitude leads to a forced phasing of all the modes which comprise the wave field (11), such that as the waves propagate down the channel there is a focussing after two wavelengths, for this wave period (the largest contourline corresponds to 1.1; the smallest, to the far right, is 0.3).

Fig. 3 shows the decay of the absolute magnitude of each of the largest five wave modes down the channel centerline for this example; clearly the higher modes (greater than, say, the third) decay rapidly (note one wavelength corresponds to 102 m) and, after long distances, only the first mode is important.

Melo and Guza (1991b) carried out a field experiment at Mission Bay, CA. The entrance channel is 1200 m long, 250 m wide, with a depth of 8 m. The jetties are sand tight, prohibiting the propagation of waves through the jetties. Pressure sensors were deployed at five locations along the centerline of the jetties as shown in Figure 4. Data was obtained during the period March 2 to April 8, 1985. Using data and parabolic model predictions, Melo and Guza determined that the effects of wave height and bottom friction on the wave height reduction along the channel were small. There was no wave breaking observed in the channel.

The effects of currents were observed to have only a small effect on the damping down the channel. The model given in the section Effects of Tidal Currents can predict the damping factor exactly;  $\Gamma$  is the imaginary part of  $\left(\sqrt{k_1^2 - \lambda_1^2}\right)$ . A variation in  $U$  of  $\pm 1$  m/s had nearly no effect on the value of  $\Gamma$ ; the variation was less than 0.3%.

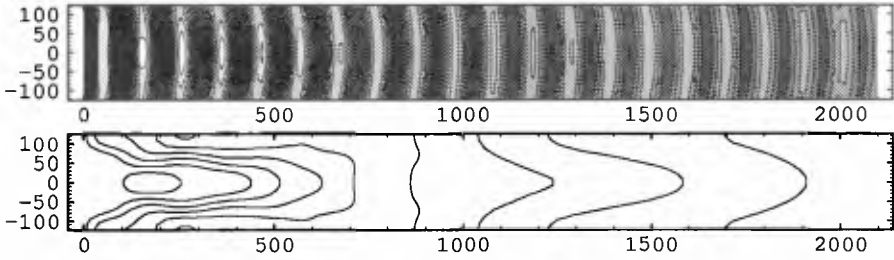


Figure 2: (a) Plane View of Instantaneous Water Surface Elevation in Channel; Ocean at the Left of Figure, Harbor to Right; (b) Absolute Value of Water Surface Elevation, Contours Intervals are 0.1

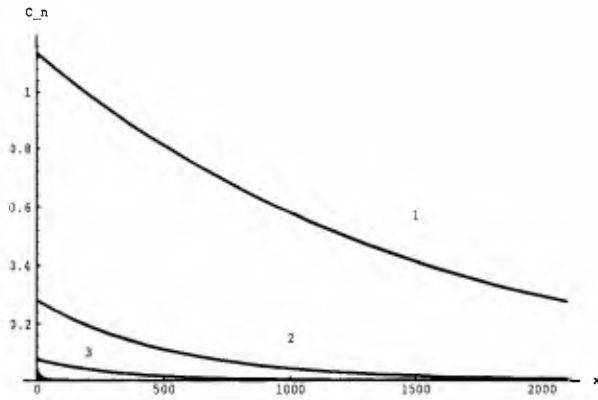


Figure 3: Decay of Each Wave Mode Down Channel (at centerline)

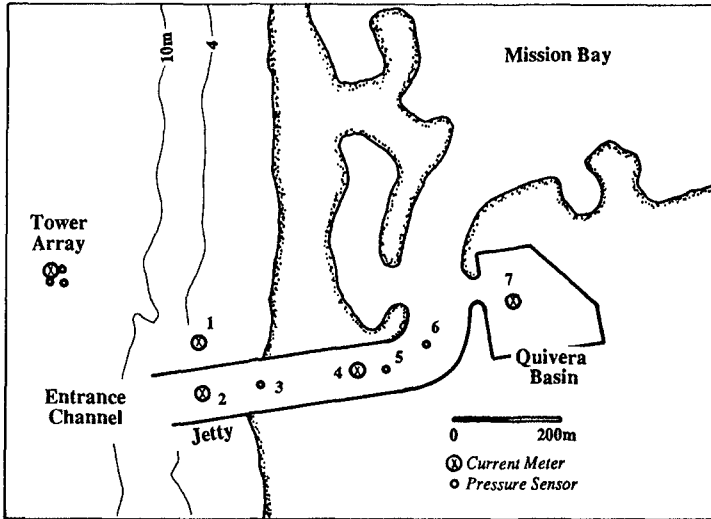


Figure 4: Pressure Sensor Locations for Mission Bay Study (from Melo and Guza, 1991b)

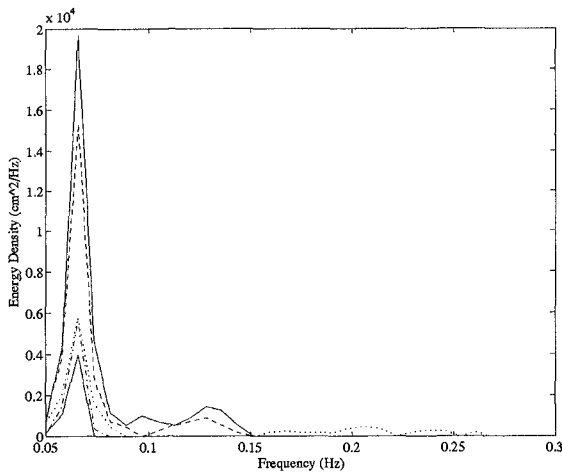


Figure 5: Wave Spectra at the Different Channel Locations (1 April, 1985; adapted from Melo and Guza, 1991b) Legend: Upper Solid Line, P2; Dashed Line, P3; Dotted Line, P4; Dash-Dot, P5; Lower Solid Line, P6.

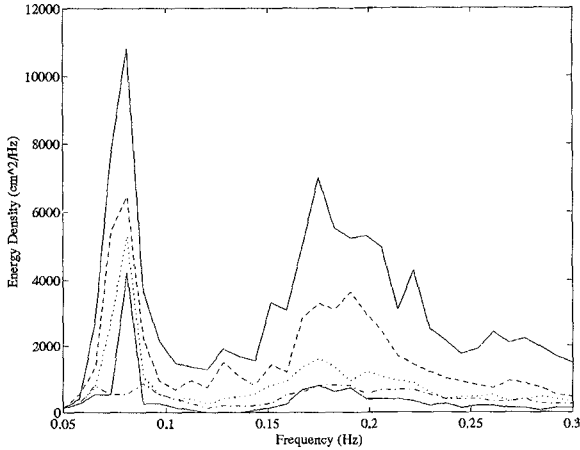


Figure 6: Wave Spectra at the Different Channel Locations (28 March, 1985; adapted from Melo and Guza, 1991b)

The wave spectra observed at the five locations in the channel by Melo and Guza on April 1, 13:31–14:40 hs, 1985 and March 28, 12:24–13:32 hs, 1985 are shown in Figures 5 and 6. Thirty three different frequencies are represented from 0.05 Hz to 0.3 Hz ( $\Delta f = 0.078$  Hz). A comparison of this model to the field data was undertaken by calculating the wave field associated with each of the 33 frequency bands (with unit amplitudes at the channel mouth). The energy densities at the first interior gage, *P2*, were then scaled to match the field data at that location. The wave heights at the other 4 gage locations were then computed from Eq. 11. These heights were then converted into energy densities and plotted. The results for each of the 33 frequency bands are shown in Figure 8 for the 1 April case. By best fit matching of the data, a smoothly varying impedance was chosen, corresponding to an impedance angle linearly varying from  $6.3^\circ$  to  $57.3^\circ$  at the highest frequency (giving  $0.004 \text{ m}^{-1} > \gamma < .04 \text{ m}^{-1}$ , from lowest to the highest frequency). The agreement between model and field data is reasonably good, giving confidence in the model for low frequencies (0.05 to 0.1 Hz; or for a range of dimensionless channel widths,  $4 < kb < 9$ ).

For the spectrum with sea and swell, March 28, the specific admittance was taken the same as for the previous case for the 10 lowest frequencies, but the higher frequencies could not be computed reasonably. The higher frequency wave in the range of 0.15 Hz to 0.30 Hz were predicted to grow down the channel.

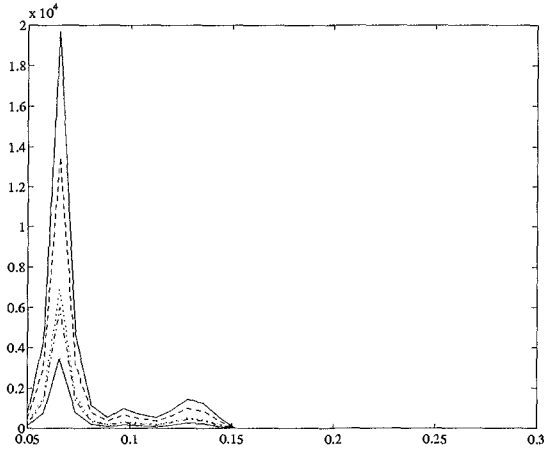


Figure 7: Computed Wave Spectra at the Different Channel Locations, April 1.

The reason for this 'growth' is the location of the focussing region shown in Fig. 2b. For the higher frequencies, this focussing region migrates down the channel, giving an apparent amplification, which is not seen in the field data. These waves (roughly  $14 < kb < 44$ ) are seriously affected by the phases imposed by the initial condition. For the lower frequency waves this was not a problem as the focussing occurred before any of the measurement points. For a realistic case, the phasing of the wave modes will be far different. In Fig. 8,  $\gamma$  was taken somewhat arbitrarily taken as  $0.007(1 - i)$  for the higher frequencies, as it was found by trial and error that the use of a complex value would reduce the amount of focussing.

As an alternative and a simpler approach to this problem, a pure exponential decay (according to Eq. 19) was tried. The wave energy density at P2 was multiplied by

$$e^{-\left(\frac{2\gamma}{2bk}\right)x} = e^{-\frac{\beta}{b}x} \quad (25)$$

where the introduction of the 2 comes about by the energy being proportional to the square of the wave height. Using the specific admittance ( $\beta$ ) of 0.139 (apparent angle of  $8^\circ$  and  $\gamma = k\beta$  ranging from  $0.005 \text{ m}^{-1}$  for the low frequency waves to  $.05 \text{ m}^{-1}$  for the highest frequency) for April 1 and 0.190 (apparent angle of  $11^\circ$ ) for March 28, gives the results in Figs. 9 and 10. For the case of the narrow banded sea state, there is almost no difference between the complete

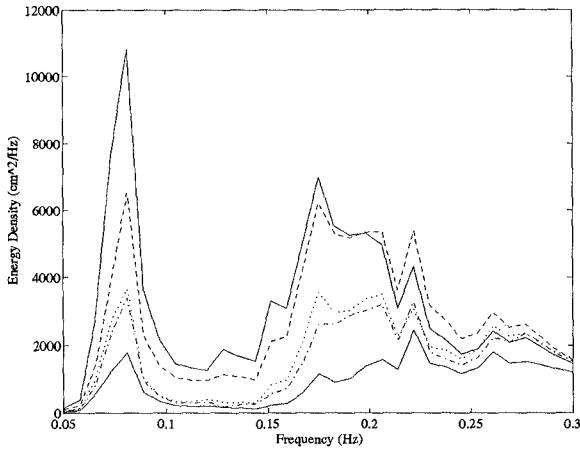


Figure 8: Computed Wave Spectra at the Different Channel Locations, March 28.

model (Fig. 7) and the exponentially decaying model. For the wide-banded seas, the frequency dependency of  $\gamma$  causes the low frequencies to decay too rapidly when compared to the field data. This can of course be improved by varying  $\gamma$  in the model. The exponential model result here is better than the complete model shown in Fig. 8, because only a single wave mode is used and the focussing can not occur.

### Conclusions

The behavior of water waves in straight channels with energy absorbing side walls, such as rubble mound jetties, can be reasonably predicted with a simple eigenfunction expansion model. For the case of Mission Bay, CA, only a very few wave modes are needed to provide an adequate description of the wave field, except for the case of the high frequencies. The absorbing sidewalls are modelled by a simple impedance boundary condition (Eq. 10), where the specific admittance  $\beta$  can be expressed as an equivalent transmission angle, *theta* from  $\beta = \sin \theta$ . The values of  $\theta$  found here are between 8 and 11°.

The complete model predicts the decay of wave spectra at Mission Bay, CA reasonably well for the low frequencies, with problems associated with focussing and the phasing of the initial condition at the higher frequencies. A simple model based on purely exponential decay (Eqs. 19 and 20) provides a useful tool for preliminary estimates of wave decay.

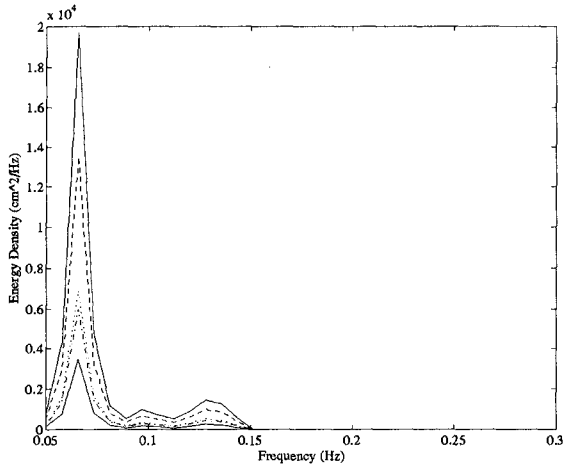


Figure 9: Exponentially Decaying Spectra at the Different Channel Locations; April 1.

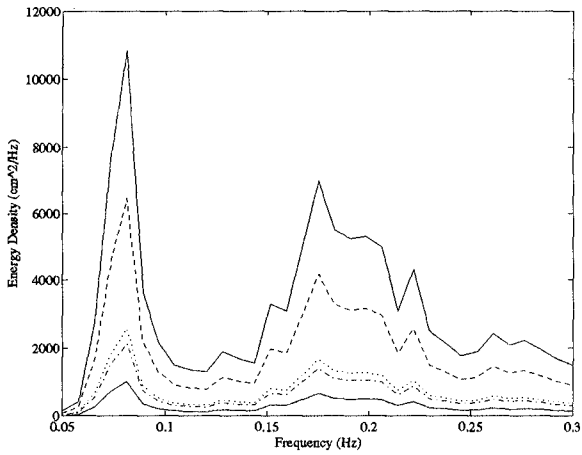


Figure 10: Exponentially Decaying Spectra at the Different Channel Locations; March 28.

### Acknowledgment

This work was partially supported by NOAA Office of Sea Grant, Dept. of Commerce, under Grant No. NA16RG0162-02 (R/OE-7). The U.S. Government is authorized to produce and distribute reprints for government purposes notwithstanding any copyright notation that may appear herein.

### Reference

- Battjes, J.A., "Wave attenuation in a channel with roughened sides," *Proc. Coastal Engineering Specialty Conference*, ASCE, 425-460, 1965.
- Behrendt, L., A finite element model for water wave diffraction including boundary absorption and bottom friction, ISVA, Tech. Univ. Denmark, Series Paper 37, 1985.
- Dalrymple, R.A., "Directional wavemaker theory with sidewall reflection," *Journal of Hydraulic Research*, 27, 1, 23-34, 1989.
- Dalrymple, R.A. and P.A. Martin, "A perfect boundary condition for parabolic water-wave models," *Proc. Royal Soc. of London, A*, 1991.
- Dalrymple, R.A., M.A. Losada and P.A. Martin, "Reflection and transmission from porous structures under oblique wave attack," *J. Fluid Mechanics*, 224, 625-644, 1991.
- Hunt, J.N., "Viscous damping of waves over an inclined bed in a channel of finite width," *Houille Blanche*, 7, 836-842, 1952.
- Isaacson, M. de St.Q, "Wave dampening due to rubblemound breakwaters," *J. Waterways, Port, Coastal and Ocean Engineering*, ASCE, 104, 4, November, 391-405, 1978.
- Losada, M.A., R.A. Dalrymple, and C. Vidal, "Water waves in the vicinity of breakwaters," *J. Coastal Research*, SI #7, 119-137, 1990.
- Melo, E. and R.T. Guza, "Wave propagation in a jettied entrance channels, I: Models" *J. Waterways, Port, Coastal and Ocean Engrg.*, ASCE, 117, 5, 471-492, 1991a.
- Melo, E. and R.T. Guza, "Wave propagation in a jettied entrance channels, II: Observations" *J. Waterways, Port, Coastal and Ocean Engrg.*, ASCE, 117, 5, 493-510, 1991b.
- Morse, P.M. and K.U. Ingard, **Theoretical Acoustics**, Princeton Univ. Press, 927pp., 1968.
- Sollitt, C.K. and R.H. Cross, "Wave transmission through permeable breakwaters," *Proc. 19th Coastal Engng. Conf.*, ASCE, Vancouver, 1827-1846, 1972.
- Sollitt, C.K. and R.H. Cross, Wave reflection and transmission at permeable breakwaters, U.S. Army Coastal Engineering Research Center, Tech. Paper 76-8, 172pp, 1976.
- Sommerfeld, A., "Mathematische Theorie der Diffraction," *Math. Annalen*, 47, 317-374, 1896.